AAPG/SEG/SPWLA HEDBERG CONFERENCE
"Fundamental Parameters Associated with Successful Hydraulic Fracturing – Means and Methods for a Better Understanding"
DECEMBER 7-11, 2014 – AUSTIN, TEXAS

A Geomechanical Approach for Microseismic Fracture Mapping

S. Mehran Hosseini, Fred Aminzadeh
University of Southern California, Mork Family Department of Chemical Engineering and Materials Science, Los Angeles, CA, USA

Abstract

Hydraulic fracturing plays an important role in economical oil and gas production from unconventional resources. It has been more than a decade since the idea of ideal bi-wing hydraulic fractures is challenged by observations from microseismic data and other sources (Rutledge et al. 2003; Warpinski et al. 2004; Agharazi et al. 2013). Most of the analysis and interpretations regarding the direction of hydraulic fracture propagation deals with associating a microseismic event with a specific step in the hydraulic fracturing process. However, based on numerous past studies, it is established that direct association, without considering reservoir geomechanics and pore pressure perturbation due to leak-off, may not be realistic. For instance induced seismicity created by waste water injection, fluid accumulation in dams, and flow in geothermal reservoirs are all cases where seismic and microseismic activities were observed in the absence of hydraulic fracturing (McClure and Horne, 2014). In this paper, using Mohr-Coulomb failure criteria, we study the change in effective stress and subsequent shear failure as the mechanism behind microseismic events. Among different mechanisms of thermal stress, pore pressure change, compaction induced stresses, and stress change around a fracture; pore pressure change and stress change around a fracture are the two main mechanisms involved in hydraulic fracturing microseismicity. By solving the pressure diffusion equation and solving for the stress field around a hydraulic fracture, we show that the pore pressure change due to leak-off can affect the reservoir in a large scale. By coupling both the pore pressure change and stress change due to fracturing, we study the expected microseismic behavior around a propagating hydraulic fracture.

We use linear elastic fracture mechanics (LEFM) to describe stress distribution around a single hydraulic fracture. The full stress field solution is valid everywhere in the domain and is a function of stress boundary conditions and fracture geometry (Anderson, 2005). Here, a full stress distribution solution for a mode I fracture where a constant pressure inside the fracture propagates the crack, is presented (Pollard and Segall, 1987):

$$S_{xx} = S^r_{xx} - (p_{Frac} - S^r_{yy})[rR^{-1}\cos(\theta - \Gamma) - 1 - a^2 rR^{-3}\sin\theta\sin 3\Gamma] \quad (4)$$

$$S_{yy} = S^r_{yy} - (p_{Frac} - S^r_{yy})[rR^{-1}\cos(\theta - \Gamma) - 1 + a^2 rR^{-3}\sin\theta\sin 3\Gamma] \quad (5)$$

$$S_{xy} = S^r_{xy} - (p_{Frac} - S^r_{yy})[a^2 rR^{-3}\sin\theta\cos 3\Gamma] \quad (6)$$

where S_{xx} is the total stress in the X direction, S_{yy} is the total stress in the Y direction, S_{xy} and S_{yx} are the shear stresses on the XY plane which are equal. S_{rxx} and S_{ryy} are the total remote stresses in the x and y direction respectively, S_{rxy} is the remote shear stress which is equal to zero in this case, a is the fracture half-length, P_{Frac} is the fracturing pressure inside the fracture which is assumed to be about 500 psi greater than the minimum vertical stress acting on the face of the fracture in this paper. $R= (r_1.r_2)^{1/2}$ and r_1, r_2, r, θ_1, θ_2, and θ as well as fracture geometry are shown in Figure 1.

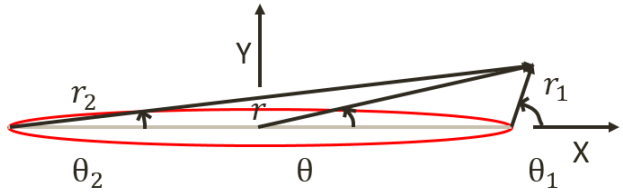

Figure 1. Fracture geometry and geometric parameters used in the full stress field solution.

Based on Anderson's faulting theory (Anderson, 1951), the magnitudes of the greatest, intermediate, and least principal total compressive stresses at depth, S_1, S_2 and S_3 respectively, can be associated with S_V, S_{hmin} and S_{Hmax} according to each faulting regime. S_V, S_{hmin} and S_{Hmax} correspond to total vertical stress, minimum, and maximum horizontal stresses, respectively. We use critically stressed crust theory to find a relationship between principal stresses in the crust. Figure 2 shows the two stress bounding limits, assuming a hydrostatic reservoir pore pressure. Mohr-Coulomb failure criteria is used to assess the extent of sheared zone around a hydraulic fracture as an indicator for potential microseismic-prone areas in the reservoir. Based on different possible stress states at 9000 and 3000 ft depths, the shape and size of the shear zones for the cases of strike-slip faulting and reverse faulting regimes in hydrostatically and highly over-pressured reservoirs for a 200 ft total length of a hydraulic fracture are shown in Figure 3. The blue area is shear-failure-prone zone for the case of a 200 ft total length of a hydraulic fracture with S_{yy} = 5220 psi and S_{xx} = 24120 psi (9000 ft depth, strike-slip faulting) in a hydrostatically pressurized reservoir (λ = 0.44). The green area is shear-failure-prone zone for the same length hydraulic fracture but with S_{yy} = 8663 psi and S_{xx} = 10350 psi (9000 ft depth, strike-slip faulting) in a highly over-pressurized reservoir (λ = 0.95). The red area is shear-failure-prone zone with S_{yy} = 3000 psi and S_{xx} = 8040 psi (3000 ft depth, reverse faulting) in a hydrostatically pressurized reservoir (λ = 0.44).

As it can be observed in Figure 3, the size of shear-failure-prone zone can be very different based on stress state and reservoir pore pressure. Subsequently, the extent and number of microseismic events around a hydraulic fracture can be very different. For instance in the case of a 200 ft long hydraulic fracture, shear-failure-prone zone for the hydrostatic pore pressure and strike-slip faulting regime case at 9000 ft depth is ~16 times higher than for the hydrostatic pore pressure and reverse faulting regime case at 3000 ft depth. So far, we discussed the cases where the matrix permeability is so low that we neglect the effect of pressure diffusion from the fracture into the formation. However, in fractured reservoirs, system permeability is much higher and the effect of pressure diffusion from fracture becomes considerable; thus we also study the effect of pore pressure increase due to leak-off from the fracture and add this mechanism to the stress perturbation due to mechanical hydraulic fracture propagation. Using typical shale properties, we conduct a sensitivity analysis for the effect of different reservoir flow properties as well as geological and geomechanical properties on the expected microseismic reservoir response and its relationship with hydraulic fracturing. The results of this study can be used for a more realistic, physics-based microseismic fracture mapping, and a better design of hydraulic fracturing process to better stimulate the reservoir and improve production.

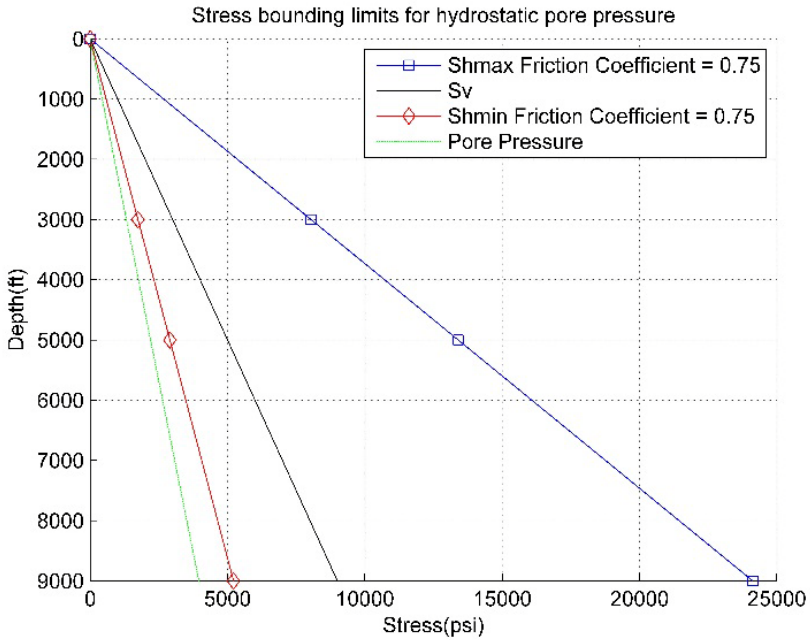

Figure 2. Stress bounding limits, assuming a hydrostatic reservoir pore pressure.

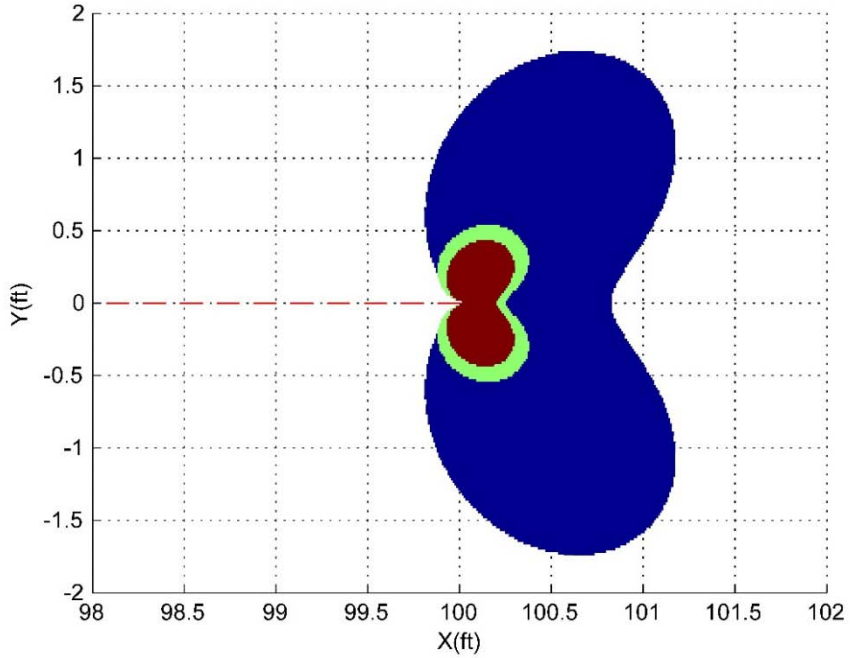

Figure 3. Shear-failure-prone zone at the tip of a 200 ft length hydraulic fracture shown with red dashed line. The blue area is the shear-prone-zone for the case with S_{yy} = 5220 psi and S_{xx} = 24120 psi (9000 ft depth, strike-slip faulting) in a hydrostatically pressurized reservoir (λ = 0.44). The green area is for the case with S_{yy} = 8663 psi and S_{xx} = 10350 psi (9000 ft depth, strike-slip faulting) in a highly over-pressurized reservoir (λ = 0.95) where the red area is for the case with S_{yy} = 3000 psi and S_{xx} = 8040 psi (3000 ft depth, reverse faulting) in a hydrostatically pressurized reservoir (λ = 0.44).

References

Agharazi, Alireza, Fengshou Zhang, Marisela Amanda Sanchez, Neal Borden Nagel, and Byungtark Lee. (2013). The Critical Role of In-Situ Pressure on Natural Fracture Shear and Hydraulic Fracturing-Induced Microseismicity Generation, SPE Unconventional Resources Conference Canada, Society of Petroleum Engineers.

Anderson, E.M. (1951). The Dynamics of Faulting and Dyke Formation with Applications to Britain. Edinburgh, Oliver and Boyd.

Anderson, T.L. (2005). Fracture mechanics: fundamentals and applications. 3rd Ed, CRC.

McClure, M. W., and R. N. Horne (2014), Correlations between formation properties and induced seismicity during high pressure injection into granitic rock, Engineering Geology, 175, 74-80.

Pollard, D.D., and P. Segall. (1987). Theoretical displacements and stresses near fractures in rock: with applications to faults, joints, veins, dikes, and solution surfaces. Fracture mechanics of rock, ed. B.K. Atkinson, 277-349.

Rutledge, J. T., & Phillips, W. S. (2003). Hydraulic stimulation of natural fractures as revealed by induced microearthquakes, Carthage Cotton Valley gas field, east Texas. Geophysics, 68(2), 441-452.

Warpinski, N. R., Wolhart, S. L., & Wright, C. A. (2004). Analysis and prediction of microseismicity induced by hydraulic fracturing. SPE Journal, 9(01), 24-33.